

MIT Open Access Articles

The perfluoropolymer upper bound

The MIT Faculty has made this article openly available. **Please share** how this access benefits you. Your story matters.

Citation: Wu, Albert X. et al. "The perfluoropolymer upper bound." *AIChE Journal* 65, 12 (June 2019): e16700 © 2019 American Institute of Chemical Engineers

As Published: <http://dx.doi.org/10.1002/aic.16700>

Publisher: Wiley

Persistent URL: <https://hdl.handle.net/1721.1/123841>

Version: Author's final manuscript: final author's manuscript post peer review, without publisher's formatting or copy editing

Terms of use: Creative Commons Attribution-Noncommercial-Share Alike



The Perfluoropolymer Upper Bound

*Albert X. Wu, James A. Drayton, Zachary P. Smith**

Department of Chemical Engineering, Massachusetts Institute of Technology, Cambridge, MA 02139

Topical heading:

Separations: Materials, Devices and Processes

Keywords:

Membrane-based separations, solubility, activated diffusion theory, perfluorocarbon

Abstract:

Perfluoropolymers have fundamentally distinct thermodynamic partitioning properties compared to those of their hydrocarbon counterparts. However, current upper bound theory assumes hydrocarbon solubility behavior for all polymers. Herein, the fundamental presupposition of invariance in solubility behavior to upper bound performance is critically assessed for perfluoropolymers and hydrocarbon polymers. By modifying solubility relationships, theoretical perfluoropolymer upper bounds are established, showing a positive shift of the upper bound front as a result of beneficial solubility selectivities for certain gas pairs, including N_2/CH_4 , He/H_2 , He/N_2 , He/CH_4 , and He/CO_2 . Within the framework of the solution-diffusion model, an analysis is presented to compare two independent approaches often pursued in efforts to surpass the polymer upper bound: (1) achieving solubility selectivity via perfluoropolymers and (2) improving diffusion selectivity via rigid hydrocarbon polymers. This analysis demonstrates the significant benefit that can be achieved by considering both the chemical composition and morphology of solid-state macromolecules when designing membrane materials.

1. Introduction

In the past few decades, polymer membranes have emerged as a promising platform for energy-efficient gas separations.¹⁻³ In these unit operations, gases are separated based on their relative differences in diffusion rates and sorption coefficients. Polymer membranes are currently used in limited industrial capacity, such as removal of CO₂ from natural gas for natural gas sweetening, nitrogen generation for On-Board Inert Gas Generation Systems (OBIGGS), and a variety of hydrogen separations in the petrochemical industry.⁴ A major challenge preventing membranes from wider industrial deployment is a general tradeoff between gas permeability and selectivity, which is described empirically by the so-called Robeson upper bound.⁵ First established in 1991 and revisited in 2008, the upper bound showed this general inverse relationship for many common gas pairs and described the best performing materials at the time, thereby setting a standard of comparison for newly developed materials.^{5,6} A theoretical analysis by Freeman revealed two pathways to surpass current limitations in membrane performance; namely, improving diffusion selectivity and/or improving sorption selectivity.⁷ Since then, researchers have focused predominantly on creating novel materials to improve diffusion selectivity,⁸⁻¹¹ while far fewer efforts have been expended on sorption selectivity.^{12,13}

Perfluoropolymers are an unusual class of polymeric materials with performance characteristics that define the upper bound front for several gas pairs. These polymers have C-F bonds instead of the more typical C-H bonds, a distinct chemical feature that influences polymer-penetrant interactions. Within the solution-diffusion framework, these modifications to polymer-penetrant interactions alter sorption selectivities, and hence, permselectivities, thereby shifting upper bound performance for certain separations.¹⁴ Readers are directed to a book chapter by Merkel that expounds on the unique solubility characteristics of perfluoropolymers and recounts a brief history of research efforts in this area.¹⁵ In the timespan between the publication of the first upper bound database in 1991 and the revisited database in 2008, a variety of new perfluoropolymers had been tested. Robeson noted that perfluoropolymers showed the highest

combinations of permeability and selectivity for all He and many CH₄ based separations, suggesting that the unique solubility behavior of perfluoropolymers was responsible for these findings.⁶

The majority of publications on novel membrane materials development in the past 30 years have focused on improving performance via diffusion selectivity by simultaneously creating stiffer polymer backbones and increasing inter-chain spacing, thus following the materials design strategy originally proposed by Freeman.⁷ While still profitable for the development of fundamental science, practically, improvements in diffusion selectivity often result in reduced mechanical integrity and increased physical aging rates.^{16,17} Therefore, this work aims to highlight potential improvements in transport properties by considering solubility selectivity as a primary consideration. Results suggest that this approach offers the ability to surpass current limitations in materials performance while simultaneously circumventing some of the key challenges associated with diffusion-selective polymers mentioned above. To this end, the permeability and selectivity of hydrocarbon polymers, partially fluorinated polymers, and perfluoropolymers were collected from literature sources. Upper bounds for non-perfluoropolymer (*i.e.*, hydrocarbon and partially fluorinated species) are established and shifted according to the theoretical framework developed by Freeman but now allowing the underlying assumption of fixed hydrocarbon solubility selectivity to be relaxed.

2. Theory & Background

Membrane separation performance is typically evaluated by determining the permeability and selectivity of certain gases in a polymer. Permeability is defined as the flux of gas through the membrane normalized by the pressure differential across the membrane and the thickness of the membrane:

$$P = \frac{Nl}{\Delta p} \quad (1)$$

where P is the permeability of a gas, N is the molar flux through the membrane, l is the membrane thickness, and Δp is the pressure differential.²

Permeability is commonly expressed in units of Barrer:

$$1 \text{ Barrer} = 10^{-10} \frac{\text{cm}^3(\text{STP}) \cdot \text{cm}}{\text{cm}^2 \cdot \text{s} \cdot \text{cmHg}} = 3.35 \times 10^{-16} \frac{\text{mol} \cdot \text{m}}{\text{m}^2 \cdot \text{s} \cdot \text{Pa}} \quad (2)$$

Gas transport through polymeric membranes is commonly described via the solution-diffusion model. Within this theoretical framework, gases sorb into the upstream face of the membrane, diffuse across the membrane along a chemical potential gradient, and then desorb from the downstream face of the membrane. From this model, permeability can be represented as the product of an effective diffusion coefficient, D , and the equilibrium sorption coefficient, S .¹⁴

$$P = DS \quad (3)$$

The units for D and S are traditionally $\text{cm}^2 \text{s}^{-1}$ and $\text{cm}^3(\text{STP}) \text{cm}^{-3} \text{cmHg}^{-1}$ respectively.

The ideal selectivity for a gas pair is defined as the permeability ratio of the faster permeating gas, A, to that of the slower permeating gas, B. Using the solution-diffusion model, the ideal selectivity, α , can be written as the product of diffusion selectivity and solubility selectivity:

$$\alpha_{A/B} = \frac{P_A}{P_B} = \frac{D_A S_A}{D_B S_B} \quad (4)$$

As mentioned previously, a major challenge in membrane separations is the inverse relationship between permeability and selectivity, which is clearly apparent from the Robeson upper bound.^{5,6} As exemplified for He/H₂ separation in Figure 1, an upper bound plot is a log-log plot of permeability and selectivity that is populated with experimental performance data for a variety of polymers. Describing the best-performing materials at the time, Robeson established empirical upper bounds for common gas pairs involving He, H₂, O₂, N₂, CO₂, and CH₄ using the following mathematical form:

$$P_A = k\alpha_{A/B}^n \quad (5.1)$$

where n and k are the slope and front factor, respectively. Robeson identified a linear relationship between n and the difference in the kinetic diameters of each gas pair.⁵

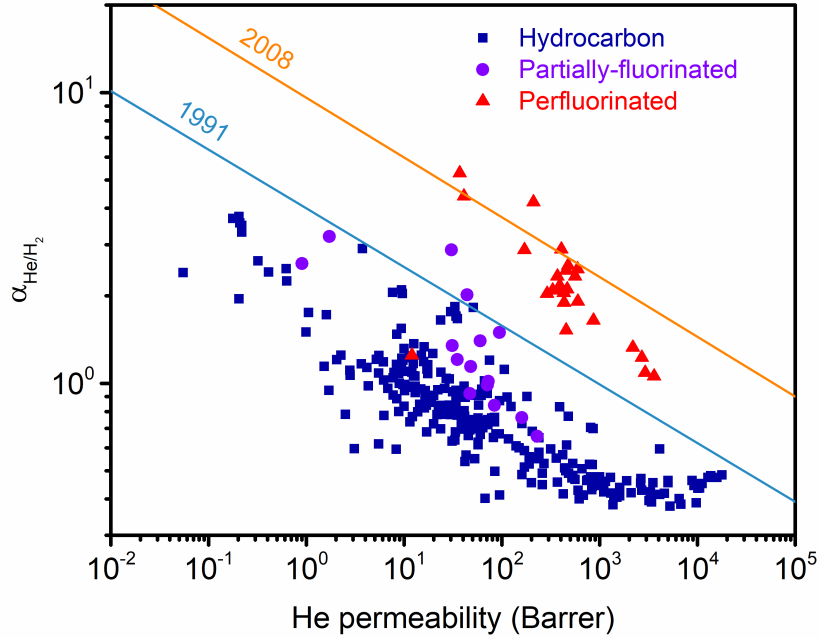


Figure 1: Example upper bound plot for He/H₂ separation. The 1991 and 2008 upper bound lines illustrate the trade-off between permeability and selectivity.^{5,6}

In 1999, Freeman derived a theoretical expression for the upper bound that matched the empirical mathematical expression originally proposed by Robeson.⁷ Freeman's approach was based on the solution-diffusion model and activated diffusion theory,^{18,19} defining the slope and front factor in terms of penetrant and polymer properties.⁷ Freeman used an equivalent form of the upper bound relationship:

$$\alpha_{A/B} = \frac{\beta_{A/B}}{P_A^{\lambda_{A/B}}} \quad (5.2)$$

where $\lambda_{A/B}$ and $\beta_{A/B}$ are altered forms for the slope and front factor, respectively.

The slope was derived to be:

$$\lambda_{A/B} = -\frac{1}{n} = \left(\frac{d_B}{d_A}\right)^2 - 1 = \left(\frac{d_B + d_A}{d_A^2}\right)(d_B - d_A) \quad (6)$$

where d_A and d_B are the gas kinetic diameters, suggesting that the upper bound slope is exclusively dependent on the gas pair and not on any characteristics intrinsic to the polymer. This result is consistent with the aforementioned observation originally described by Robeson.⁵

The front factor was derived to be:

$$\beta_{A/B} = k^{-\frac{1}{n}} = \frac{S_A}{S_B} S_A^{\lambda_{A/B}} \exp\left(-\lambda_{A/B} \left(b - f \frac{1-a}{RT}\right)\right) \quad (7)$$

where S_A and S_B are the solubility coefficients for gases A and B, and a , b , and f are parameters resulting from the application of activated diffusion theory.

To estimate the solubility and solubility selectivity (S_A/S_B) of gas in the polymer, penetrant partitioning is viewed as a two-step process, consisting of a condensation-like step of the gas adsorbing onto the polymer followed by mixing of the penetrant into the polymer matrix.^{14,20} These effects can be generalized by correlating the sorption of penetrants with some thermodynamic potential, such as the Lennard-Jones well depth of a penetrant, ε_A/k :²

$$\ln(S_A) = M + N \frac{\varepsilon_A}{k} \quad (8)$$

where M and N are parameters fit from experimental data on solubility for various penetrants. Freeman used values of $M = -9.84$ and $N = 0.023$ for all polymers, in units of $\text{cm}^3(\text{STP}) \text{cm}^{-3} \text{cmHg}^{-1}$, based on established correlations for hydrocarbon species.

The other parameters, a , b , and f , are a result of the application of activated diffusion theory, using Arrhenius behavior to describe the diffusion coefficient based on the activation energy of diffusion, E_D , an Arrhenius prefactor, D_0 , the ideal gas constant, R , and absolute temperature, T :¹⁸

$$D_A = D_{0,A} \exp\left(-\frac{E_{D,A}}{RT}\right) \quad (9)$$

The parameters a and b originate from the linear free energy relationship proposed by Barrer²¹:

$$\ln(D_{0,A}) = a \frac{E_{D,A}}{RT} - b \quad (10)$$

Freeman used values of $a = 0.64$ for all polymers and $b = 9.2$ or 11.5 for rubbery or glassy polymers, respectively, in units of $\text{cm}^2 \text{s}^{-1}$ for the diffusion coefficient.

The f parameter originates from the Brandt model relating the diffusion activation energy to the gas kinetic diameter, which describes the energy required to open a transient gap for a molecular jump to occur between free volume elements²²:

$$E_{D,A} = cd_A^2 - f \quad (11)$$

where c and f are constants that relate to the size-sieving ability of the polymer. The c parameter is related to backbone stiffness and acts as an energy scaling factor with respect to the penetrant diameter squared, and the f parameter is related to inter-chain packing. The quantity $\sqrt{f/c}$ can be interpreted as a rough estimate of the average chain spacing. Freeman calculated a best-fit f value of 52.7 kJ mol^{-1} for the 1991 upper bounds from a least squares regression of theoretical and experimental $\beta_{A/B}$ values across all gas pairs considered.⁷

Freeman's definitions for $\lambda_{A/B}$ and $\beta_{A/B}$ allow for theoretical predictions of the slopes of the upper bounds with no adjustable parameters and front factors with two adjustable parameters: f , relating to the inter-chain spacing, and S_A/S_B , relating to the solubility selectivity of the gases in the polymer. Since $\lambda_{A/B}$ theoretically is not be affected by polymer materials characteristics, these parameters represent the two major pathways towards increasing the value of the front factor and therefore improving the separation performance for polymeric membranes.

3. Analysis Procedure

This analysis focuses on the theoretical shifts to the upper bound fronts through the modification of the solubility terms in Equation 14. Non-perfluoropolymer upper bound fronts were re-fit from an updated

Robeson's database excluding perfluoropolymer data points to establish a clear baseline for this analysis.²³ The solubility correlation parameters were adjusted for perfluoropolymers while retaining the fitted f values from the non-perfluoropolymer upper bounds. By doing so, this procedure illustrates the potential improvements to using perfluoropolymers under the key assumption that fluorine functionality has no other effect on transport performance other than adjusting gas-polymer molecular partitioning. It should be noted that some recent data on new diffusion-selective polymers have been reported with property sets that surpass certain upper bounds.^{24,25} There are a limited number of these polymers, and they show beneficial upper bound performance for O₂/N₂, CO₂/CH₄, H₂/N₂, and H₂/CH₄ separations, which are not the primary consideration for this work. Therefore, we have chosen not to include these polymers in our analysis, thereby allowing us to use a widely accepted and published database of separation property sets.

a. Modifications from previous analysis

The analysis originally considered by Freeman was derived using a form of the linear free energy relationship proposed by Barrer.²¹ However, an alternative mathematical form has also been proposed by van Amerongen.²⁶ In 2005, Prabhakar considered the linear free energy relationships proposed by van Amerongen (Equation 12.1) and Barrer (Equation 13.1) respectively:²⁷

$$\ln(D_0) = a \frac{E_D}{R} - b \quad (12.1)$$

$$\ln(D_0) = a' \frac{E_D}{RT} - b' \quad (13.1)$$

When substituting these expressions into the Arrhenius diffusion relationship, we arrive at the following distinct definitions for diffusion coefficients:

$$D = \exp\left(a \frac{E_D}{R} - b\right) \exp\left(-\frac{E_D}{RT}\right) \quad (12.2)$$

$$D = \exp(-b') \exp\left(\frac{(a' - 1)E_D}{RT}\right) \quad (13.2)$$

Prabhakar argued against the use of the Barrer form of the linear free energy relationship because it would require a fixed intercept of b' when plotting $\ln(D)$ vs. $1/T$, regardless of the polymer-penetrant system, while conversely, the van Amerongen form would allow for an intercept that depended on the polymer-penetrant system. The null hypothesis of a fixed intercept regardless of the polymer-penetrant system was tested through a two-factor analysis of variance (ANOVA) without replication using van Amerongen's data (See SI Section B).²⁶ The variance in the intercept was found to be statistically significant when considering both polymer composition and gas selection for a separation based off both critical F and p -values, thus suggesting the van Amerongen form of the linear free energy relationship should be used for this analysis. Prabhakar reported values of $a = 0.00203$ and $b = 8.3$ for rubbery polymers and van Krevelen reported $b = 11.5$ for glassy polymers.^{27,28} This aforementioned modification leads to a slightly modified form of $\beta_{A/B}$:

$$\beta_{A/B} = \frac{S_A}{S_B} S_A^{\lambda_{A/B}} \exp\left(-\lambda_{A/B} \left(b - f \frac{1 - aT}{RT}\right)\right) \quad (14)$$

b. Necessity of non-perfluoropolymer upper bounds

New non-perfluoropolymer upper bounds were determined by eye for this analysis, following a similar procedure to that used by Robeson in estimating the original 1991 and 2008 upper bounds.^{5,6} An example highlighting the need for the creation of distinct upper bounds based off chemical structure is shown in Figure 2a, where there is a significant difference in the location of the upper bound front depending on whether or not perfluorinated polymers are considered. A particular distinction is made for this work in describing the new upper bounds as “non-perfluoropolymer” instead of “hydrocarbon”. This terminology is chosen because many partially fluorinated polymers (*e.g.*, 4,4'-(hexafluoroisopropylidene)diphthalic anhydride (6FDA) based polyimides) have shown sorption behavior more similar to that of hydrocarbon polymers than perfluoropolymers.²⁹ An exception to this distinction is made for Viton[®] E60 and Viton[®] GF, both highly fluorinated elastomers (65 wt% F and 75 wt% F respectively), since they display sorption behavior consistent with perfluoropolymers.³⁰ A remarkable example of how transport properties for

partially fluorinated Viton[®] polymers more closely align to those of perfluoropolymers is noted for the He/H₂ upper bound presented in Figure 3a. In this example, Viton[®] polymers are the only non-perfluorinated polymers exceeding the non-perfluoropolymer upper bound.

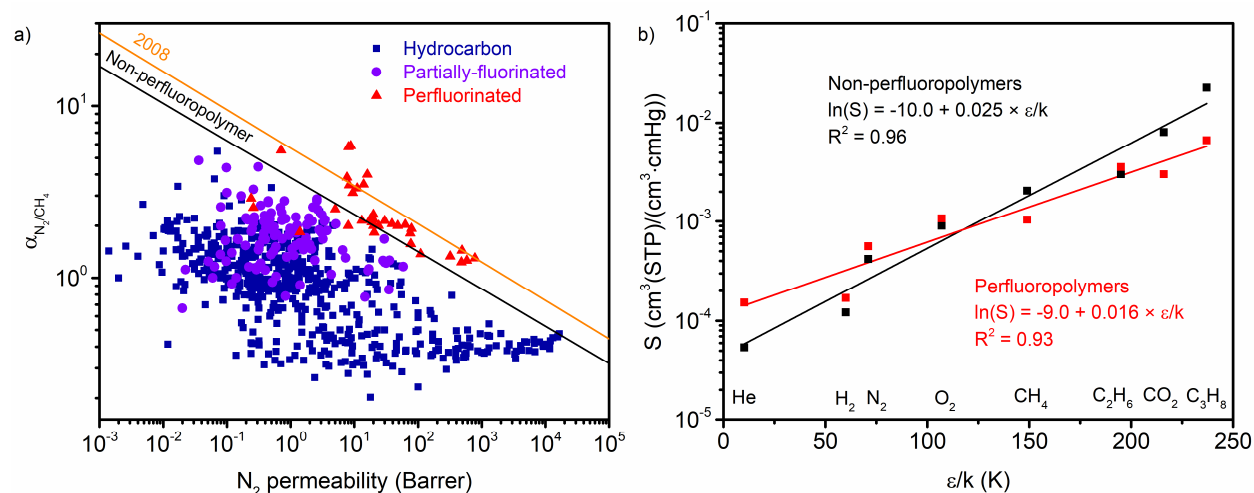


Figure 2: a) A representative upper bound plot with data points identified as hydrocarbon, partially-fluorinated, and perfluorinated. Non-perfluoropolymer upper bounds are established for this work because the upper bound database includes a large amount of perfluoropolymer data. b) Best-fit solubility correlation parameters when comparing non-perfluorinated and perfluorinated polymers at 35°C and 1 atm.

c. Selection of molecular diameters

It has been previously noted that theoretical upper bounds calculated from Freeman’s approach match poorly with Robeson’s experimental upper bound plots, primarily as a result of the use of kinetic diameters for the analysis.³¹ This inconsistency has prompted studies into using new sets of diameter definitions suitable for describing diffusion through polymeric media such as the “Dal-Cin” and the “permeability correlation” diameters.^{31,32} For this study, the so-called “diffusion” diameters were employed.²³ These diameters are calculated from a least squares minimization approach that optimizes a fit for molecular diameters based on correlations from a large database of gas diffusion coefficients in polymer membranes.²³ This diameter set assumes a fixed CH₄ diameter of 3.817 Å (1 Å = 10⁻¹⁰ m) as a basis for the least squares

minimization because CH₄ is nearly spherical and there is little variation in literature-reported diameters.³² For this analysis, diffusion diameters resulted in the lowest sum-of-squared-residuals when comparing between predicted and non-perfluoropolymer $\lambda_{A/B}$ values for all gas pairs considered in this analysis. Other diameter sets considered included the kinetic, Dal-Cin, Teplyakov-Meares, Lennard-Jones, permeability correlation, Lennard-Jones collision, and effective diameters.^{31–38}

d. Calculation of individual f values for each gas pair

With the non-perfluoropolymer upper bounds and the diameter sets established, f values were calculated for each gas pair to exactly match the upper bound fit to the empirical non-perfluoropolymer upper bounds. Fitting a singular best-fit f value across all gas pairs resulted in significant variability to upper bound fits, suggesting that this simplification would severely limit the predictive applicability of the theory developed in this paper. Therefore, f values are defined for each gas pair.

e. Adjustment in solubility correlation

The non-perfluoropolymer upper bounds were shifted by adjusting the S_A and S_B values in Equation 14 according to observed changes in M and N between non-perfluoropolymers and perfluoropolymers. The changes in correlation parameters were determined from a collection of published non-perfluorocarbon and perfluorocarbon sorption coefficients at or near standard testing conditions of 35°C and 1 atm (see Table S4), as shown in Figure 2b. The parameters for the non-perfluorocarbons were $M = -10.0 \pm 0.3$ and $N = 0.025 \pm 0.002$ and the parameters for the perfluorocarbons were $M = -9.0 \pm 0.3$ and $N = 0.016 \pm 0.002$. These parameters were determined by performing linear regression on the natural log of the sorption coefficient with respect to the Lennard-Jones temperature for a variety of common gases. The natural log of the gas solubility coefficient is commonly correlated, to good accuracy, with respect to other thermodynamic properties of gases such as critical temperature or boiling temperature (see Equation 8).³⁹ The Lennard-Jones temperature was chosen as the correlation variable because it originates from Lennard-Jones potential energy well depth, while other measures of condensability such as critical and boiling

temperature can be influenced by the strength of the intermolecular forces between individual gas molecules. The noted change in gas solubility and solubility selectivity between non-perfluoropolymers and perfluoropolymers is hypothesized to be the basis for the observed improvement in separation performance shown by perfluoropolymers for certain gas pairs.

4. Results

a. The perfluoropolymer upper bound

The above analysis procedure was implemented on gas pairs (He/H₂, He/CO₂, He/N₂, He/CH₄, and N₂/CH₄) where perfluoropolymer performance was particularly notable. Figures 3a-e present upper bound plots for these gas pairs. Included on each plot are permeabilities and selectivities for hydrocarbon, partially fluorinated, and perfluorinated polymers, and two distinct upper bounds are shown to represent the non-perfluoropolymer and perfluoropolymer upper bounds. The slope and front factor for each upper bound are listed in Table 1. The front factors for the perfluoropolymer upper bounds are significantly increased when solubility selectivities are made in accordance with empirical trends reported in the literature while retaining the non-perfluoropolymer f value.¹⁵

Gas pair	n , non-perfluoropolymer and perfluoropolymer	k , non-perfluoropolymer (Barrer)	k , perfluoropolymer (Barrer)
He/H ₂	-4.6	786	18,700
He/CO ₂	-1.6	5,100	79,500
He/N ₂	-1.0	19,900	85,800
He/CH ₄	-0.8	11,100	67,600
N ₂ /CH ₄	-4.6	508	19,900

Table 1: Tabulation of n (slopes) and k (front factors) for the gas pairs analyzed.

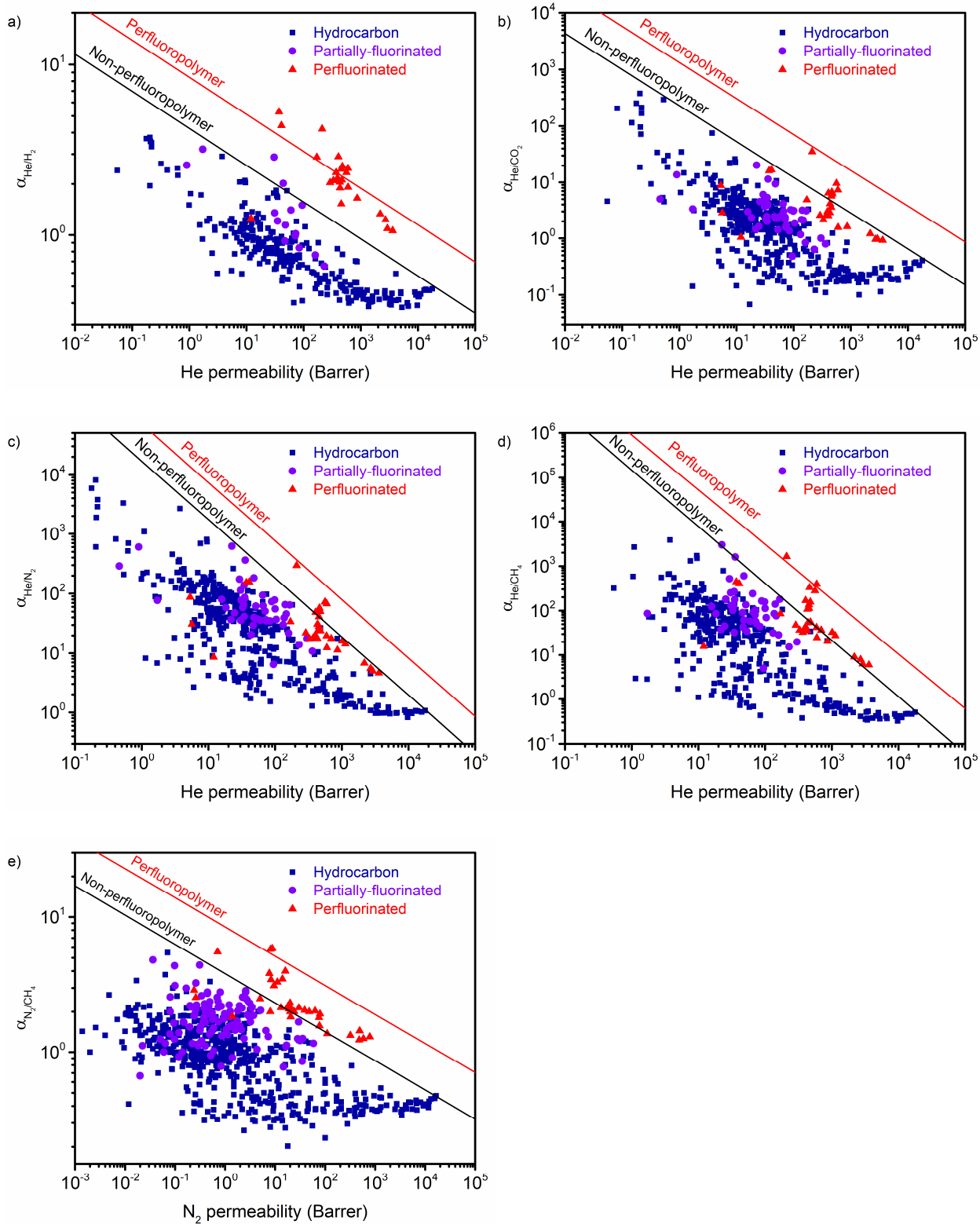


Figure 3: Upper bound plots showing the non-perfluoropolymer and perfluoropolymer upper bounds: a) He/H₂ b) He/CO₂ c) He/N₂ d) He/CH₄ e) N₂/CH₄

When comparing experimental perfluoropolymer data points with the perfluoropolymer upper bounds, there are cases where the perfluoropolymer upper bound approximately matches data for the best observed performance of known perfluoropolymers (He/CO₂, He/N₂, He/CH₄) and cases where experimental data surpasses the shifted upper bound (He/H₂, N₂/CH₄). In the most general sense, the perfluoropolymer upper bound represents the potential separation performance of the best performing non-perfluorinated polymers if they were to theoretically retain their backbone stiffness and inter-chain spacing (c and f values from Equation 11) while improving their sorption selectivities to those of perfluoropolymers. This interpretation implies that perfluoropolymers with property sets below the shifted upper bound would have a hypothetical hydrocarbon counterpart that exhibits separation performance below that of the non-perfluoropolymer upper bound. Conversely, perfluoropolymers at or surpassing the shifted upper bound are able to take advantage of perfluoropolymer solubility selectivity while simultaneously possessing size-sieving properties greater than or equal to that of the best non-perfluoropolymers for these gas pairs.

There are two subclasses of perfluoropolymers that either define or surpass the perfluoropolymer upper bound for the gas pairs considered in Figure 3: various Nafion[®] block copolymers and glassy dioxolane-based perfluoropolymers. Nafion[®] polymers are well-known for their unique packing structure due to their amphiphilic side chains. After wetting and drying of the polymer, the hydrophilic sulfonated side chains are believed to form ionic clusters within the matrix, causing the hydrophobic portion of the perfluoropolymer to pack irregularly about the clusters.⁴⁰ The notable glassy dioxolane-based perfluoropolymers are recently developed polymers of perfluoro-2-methylene-1,3-dioxolane (poly(PFMD)) and perfluoro-2-methylene-4-methyl-1,3-dioxolane (poly(PFMMD)), as well as PFMD-PFMMD block copolymers with varying block lengths.^{12,13} These dioxolane-based polymers possess cyclic structures in their backbones that frustrate packing and demonstrate glass transition temperatures ranging from 123°C to 135°C.^{12,13} Therefore, the resulting packing structure of these two subclasses of perfluoropolymers leads to good diffusion selectivity performance.⁴⁰ Such a finding reveals that it is

possible to develop materials that have solubility selectivities and size-sieving behavior that is both complementary and beneficial in surpassing property sets of conventional hydrocarbon polymers.

b. Comparison of diffusivity and solubility selectivity effects on shifting the upper bound

A helpful exercise is to consider improvements that have been made in separation performance since the publication of the 1991 upper bounds for perfluorinated and non-perfluorinated polymer structures. These performance improvements can be quantified by comparing the f values for the 1991 upper bounds with the newly fitted f values for the non-perfluoropolymer upper bounds and the “effective f ” values for the perfluoropolymer upper bounds. In this study, the “effective f ” values are defined as the calculated f values necessary to replicate the perfluoropolymer upper bound front while retaining non-perfluoropolymer solubility selectivity. In other words, the effective f for a gas pair is the f value required to shift the non-perfluoropolymer front to match that of the perfluoropolymer upper bound. Table 2 shows the newly fitted f values and the effective f values for the five gas pairs considered to match the non-perfluoropolymer and perfluoropolymer upper bounds, respectively, as previously shown in Figure 3a-e. The effective f values are between 15-29% greater than the non-perfluoropolymer f values, depending on the gas pair, with an average increase of 20%.

A similar procedure as described previously was used to calculate f values for the 1991 upper bounds. By doing so, a qualitative measure of the improvement in gas separation performance between 1991 and the current non-perfluoropolymer upper bounds could be established. The 1991 upper bounds were chosen as a baseline comparison, as opposed to the 2008 upper bounds, because the only perfluoropolymer data point at the time (Nafion[®] 117) was considered to be an outlier and was not included in the upper bound analysis.⁵

Table 2 presents the percentage increase in calculated f values from 1991 to the current non-perfluoropolymer upper bounds for the analyzed gas pairs. For these separations (*e.g.*, He/H₂, He/CO₂, He/N₂, He/CH₄, N₂/CH₄), f values shift between -1.7% and 19%. Note that the -1.7% shift for He/H₂ separation results from our decision to group Viton[®] elastomers with perfluoropolymers. Viton[®] was

originally included in the 1991 upper bound, and to date, there have been no reported property sets for non-perfluorinated polymers that have surpassed the He/H₂ separation performance of Viton[®].³⁰ As for the other gas pairs, this analysis reveals that mild improvements to separation performance have been made using synthetic design strategies that do not include perfluorinated polymers.

Conversely, Table 2 also presents a comparison of the increase in f values for the newly fitted non-perfluoropolymer upper bounds and the effective f values. In this case, significant shifts in f values between 14.9% and 28.8% are observed for the gas pairs analyzed. This remarkable finding quantitatively demonstrates the benefit to using perfluoropolymers for the five primary separations analyzed in this work. Despite nearly three decades of membrane research since the publication of the 1991 upper bound, there have been no successful design strategies for non-perfluorinated polymers capable of achieving the same performance improvements as those obtained through the use of perfluoropolymers.

A full list of f values for the 1991 upper bounds and the newly fitted non-perfluoropolymer upper bounds are compiled in Table S5 along with the corresponding percent change in f values. The newly fitted non-perfluoropolymer f values shift between -1.7% and 106% compared to the 1991 f values, depending on the gas pair, with an average increase of 27%. Of note, the two separations with the greatest improvements in non-perfluorinated property sets are CO₂/CH₄ and O₂/N₂ separations. Unlike all other separations tabulated, these separations benefit from both diffusion and solubility selectivities. For example, in the case of CO₂/CH₄ separation, CO₂ is both smaller than CH₄ and more soluble than CH₄ in polymers, thereby resulting in favorable diffusion selectivities and solubility selectivities, and hence, permselectivities. Conversely, for all of the separations enhanced through the use of perfluoropolymers, solubility selectivity is intrinsically unfavorable. For example, in the case of He/H₂ separation, He is less soluble than H₂ in polymers, thereby resulting in unfavorable solubility selectivities.^{29,41} Therefore, from the standpoint of the solution-diffusion model, perfluoropolymers are attractive for separations that benefit from weak solubility selectivities (*i.e.*, solubility selectivities closer to unity). Heuristically, Table S5 highlights the importance

of considering both molecular size and polymer-penetrant interactions when choosing a polymer for a given separation.

Gas pair	f value		Increase in f value	
	f for non-perfluoropolymer upper bound (kJ/mol)	Effective f for perfluoropolymer upper bound (kJ/mol)	Increase in f , 1991 f to non-perfluoropolymer f	Increase in f , non-perfluoropolymer f to effective f
He/H ₂	79.9	102	-1.7%	27.1%
He/CO ₂	84.1	103	19%	22.3%
He/N ₂	67.2	77.2	5.0%	14.9%
He/CH ₄	70.3	82.6	8.4%	17.6%
N ₂ /CH ₄	87.0	112	-	28.8%

Table 2: Actual and effective f values and relative increases from baseline comparisons. There was no N₂/CH₄ upper bound reported by Robeson in 1991.⁵

Figures 4a-c present upper bound plots for He/CH₄, H₂/CH₄, and CO₂/CH₄. The line labeled “1991” is the upper bound front originally described by Robeson. Accompanying values of f , M , and N required to obtain this fit are provided as a reference. The non-perfluoropolymer upper bound, which maintains an identical M and N value to that of the 1991 upper bound but a modified value of f is labeled as “Non-perfluoropolymer”. This change in f corresponds to the shift in state-of-the-art performance for non-perfluoropolymers, as described previously. The final line, labeled “1991 Shifted”, presents f values characteristic of upper bound non-perfluoropolymers in 1991, but with the solubility relationship coefficients, M and N , shifted to hypothetically account for solubility behavior that is expected for perfluoropolymers according to the solubility terms in Equation 14. For He/CH₄, modifying the 1991 upper bound by only changing the analysis to consider perfluoropolymer solubility characteristics results in a greater shift to the upper bound front than that observed for the present non-perfluoropolymer upper bound.

The same qualitative findings are observed for He/H₂, He/CO₂, He/CH₄, and N₂/CH₄ as well. For H₂/CH₄, which is shown in Figure 4b, the adjustment to perfluoropolymer solubility coefficients resulted in an improvement surpassing the 1991 baseline but did not reach the current performance limit of the non-perfluoropolymer upper bound. Lastly, there are general cases in which the use of the perfluoropolymer solubility correlation negatively impacts performance. One commonly studied gas separation that does not benefit from the sorption behavior of perfluoropolymers is CO₂/CH₄. An illustration of this behavior is shown in Figure 4c. In this case, the more strongly-sorbing penetrant (*i.e.*, CO₂) also has a smaller diameter than that of the other component (*i.e.*, CH₄), resulting in a lowered upper bound front. This penetrant size/solubility argument can be used to predict the effects of solubility changes on the upper bound position for all other gas pairs.

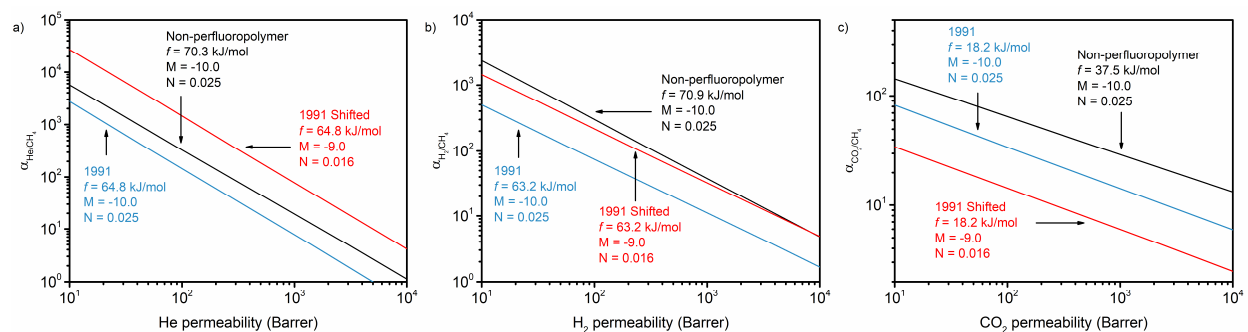


Figure 4: Comparison in the shifts of the upper bound plots from 1991 by changing either f or the characteristic solubility correlations for non-perfluoropolymers and perfluoropolymers. Results are shown for: a) He/CH₄ b) H₂/CH₄ c) CO₂/CH₄

c. Prediction of upper bound fronts from penetrant properties

A key challenge in the membrane field is the ability to predict performance limits for separations where little to no experimental data exists. Such limitations often preclude the use of process modeling to incorporate membranes into the design of separations processes. On the contrary, however, many thermally-driven separations, such as distillation, have abundant accessible datasets and tested models to ensure good predictive capabilities when designing new chemical plants. An interesting consequence of our work is the

ability to leverage theory to predict membrane separation performance for less well-studied separations. Of particular importance is a correlation that can be gleaned from the compilation of f values for individual gas pairs, as shown in Figure 5a for the non-perfluoropolymer upper bounds. When plotting $\ln(f)$ versus $\lambda_{A/B} \times S_A/S_B$ for each gas pair, there is a resulting linear correlation with a R^2 value of 0.655 and a Pearson correlation coefficient of -0.809 . A F-test of overall significance was performed with the null hypothesis stating that the fit matches the reduced model containing parameters for the intercept only. The calculated F-value for this fit was 20.9 and the critical F-value, with degrees of freedom corresponding to a 2 parameter fit and 13 observations, was equal to 4.84 for $p = 0.05$. Since the calculated F-value is larger than the critical F-value, the null hypothesis was rejected in favor of the full model containing parameters for one independent variable and the intercept, suggesting some physical meaning for this trend.⁴²

A potential interpretation is that $\lambda_{A/B}$ and the predicted value of S_A/S_B serve as proxies for diffusion and actual solubility selectivities based exclusively on correlations with well-known penetrant properties. Therefore, a larger product of the two terms represents, in general, a more efficient separation with higher selectivities because the separation is aided by properties intrinsic to the penetrants (*i.e.*, He/CO₂ is the least efficient, while CO₂/CH₄ is the most efficient). However, our interpretation of a unique f value for every gas pair is contrary to the Brandt model (*cf.*, Equation 11) where a polymer possesses a singular f value, which is seen as an intrinsic property related to the inter-chain spacing of the polymer.²² Therefore, we chose to carefully apply these predictions with the knowledge that additional theory must still be developed to fully understand the fundamental origins underlying our approach.

The obvious application of this correlation is to predict present day f values for gas pairs of interest that were not considered in this work. In doing so, new upper bounds can be predicted. Ethylene/ethane (C₂H₄/C₂H₆) and propylene/propane (C₃H₆/C₃H₈) upper bound limits have been previously established, albeit using the Lennard-Jones and Lennard-Jones collision diameters respectively.^{35,36,43,44} When our analysis was repeated using the respective diameter sets for each separation, the predicted f values are 72.1 kJ mol⁻¹ for ethylene/ethane and 66.0 kJ mol⁻¹ for propylene/propane. The original and current predicted

non-perfluoropolymer upper bound fronts with the original data sets are shown in Figures 5b-c, where a modest shift in the upper bound front is predicted. It should be noted that the trend shown in Figure 5a reflects the current progress in polymer membrane performance and should be updated as upper bound front factors increase over time with the development of new materials. Predicted perfluoropolymer upper bounds, based off of the predicted non-perfluoropolymer upper bounds, were calculated using the f values following the procedure outlined in section 3 and are shown in Figures 5b-c, predicting essentially no shift for C_2H_4/C_2H_6 and a negative shift for C_3H_6/C_3H_8 . Examining equation 14 and Figure 2b, this outcome can be attributed to a decrease in $S_A^{\lambda_{A/B}}$ when switching from hydrocarbon to perfluoropolymer solubility for these gas pairs. In the case of C_2H_4/C_2H_6 , there is no shift in the front factor because the decrease in $S_A^{\lambda_{A/B}}$ is approximately equal to the increase in S_A/S_B , while in the case of C_3H_6/C_3H_8 , the negative shift is due to the predominant decrease in $S_A^{\lambda_{A/B}}$ over the increase in S_A/S_B . This effect scales primarily with the condensability of gas A, revealing limiting cases where perfluoropolymers would not improve performance even for certain gas pairs that do follow the size/solubility argument presented in section 4b.

Figure 5d shows the predicted non-perfluoropolymer and perfluoropolymer upper bounds for H_2/C_3H_6 , an industrially important separation for olefin recovery, again using the Lennard-Jones collision diameter for this analysis.^{45,46} From the predicted upper bound fronts, it is expected that hydrogen separation from olefin streams could greatly benefit from the use of perfluoropolymers. The ability to predict upper bound fronts for gas pairs with no data points allows for a rough estimate of performance and suggests pathways for improvement. However, this approach must be used with caution, as limited data is currently available to test the key assumptions outlined in this work.

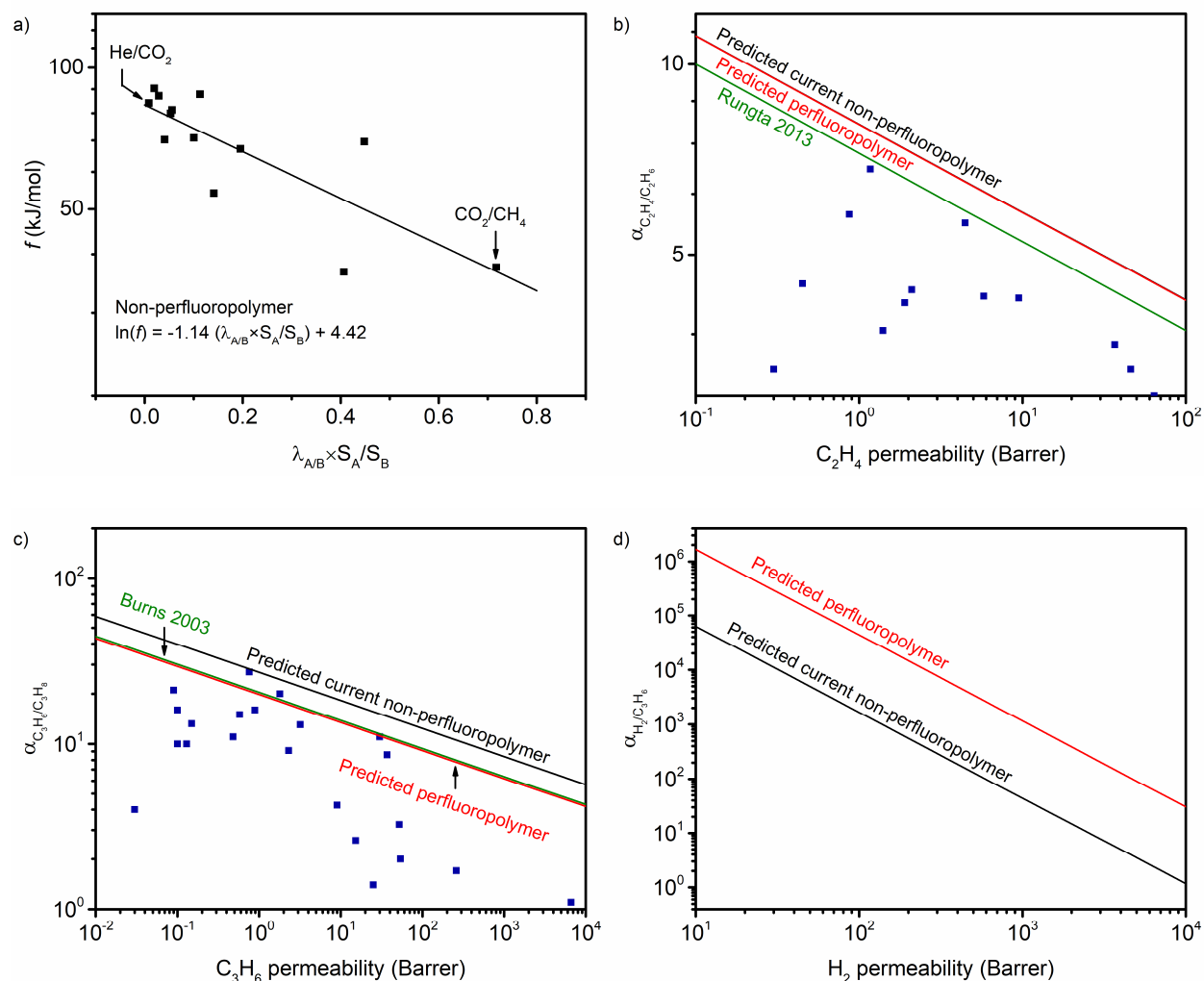


Figure 5: a) Semi-log plot showing the correlation between $\lambda_{A/B} \times S_A/S_B$ and non-perfluoropolymer upper bound f values. b) The previous upper bound, predicted current non-perfluoropolymer upper bound, and predicted perfluoropolymer upper bound for C_2H_4/C_2H_6 separation.⁴³ The two predicted upper bounds are essentially overlapping. c) The previous upper bound, predicted current non-perfluoropolymer upper bound, and predicted perfluoropolymer upper bound for C_3H_6/C_3H_8 separation.⁴⁴ d) Predicted current non-perfluoropolymer upper bound and perfluoropolymer upper bound for H_2/C_3H_6 separation.

d. Promising future gas separation applications for perfluoropolymers

While the five gas pairs analyzed were selected because of the known performance improvements that result from using perfluoropolymers, there are other separations where modifications to solubility selectivity

presents a benefit. In particular, He/O₂ and H₂/CH₄ have similar intrinsic advantageous metrics of relative molecular sizes and solubilities for their respective gas pairs that could benefit from the use of perfluoropolymers. Following the analysis procedure outlined in section 3, Figures 6a-b demonstrate the predicted shift in upper bound performance that can be achieved using perfluoropolymers for these separations. Interestingly, in contrast to our predictions, currently available data indicates that perfluoropolymers exhibit nearly the same performance as that of the best performing non-perfluoropolymers. In the case for He/O₂ separation, it has been experimentally shown that perfluorocarbon liquids have anomalously high sorption capacity for O₂, which would lower the solubility selectivity and result in depressed separation performance.⁴⁷ In the case of H₂/CH₄, it is possible that similarities in the chemical composition between H₂ and CH₄ result in H₂ having anomalous interactions with fluorocarbons, similar to that of CH₄ with C-F bonds, again resulting in lower solubility selectivity and separation performance than predicted by our solubility correlations.^{48,49} Note that in Figure 2b, H₂ and CH₄ are the two gases that deviate the most significantly from our solubility correlation. Currently, H₂/CH₄ separation represents an important challenge in refinery off-gas purification, and while He/O₂ separation is currently not practiced in industry, it could become useful in the future as helium-containing natural gas resources continue to diminish.^{2,50} Perfluoropolymers also show promise in improving H₂/C₃H₆ separations for olefin recovery from thermal cracking or off-gas streams, as shown in Figure 5d.^{45,46} Additionally, perfluoropolymers, which possess a nano-confined packing structure with unique electronic interactions stemming from their highly polarized C-F bonds,^{51,52} could also be of interest for a variety of valuable isotope separations such as H₂/D₂ separation for the production of “heavy drugs” associated with decreased pharmacokinetics and fewer side effects, or for ³He/⁴He separation for medical applications related to imaging of the human lungs.^{53,54}

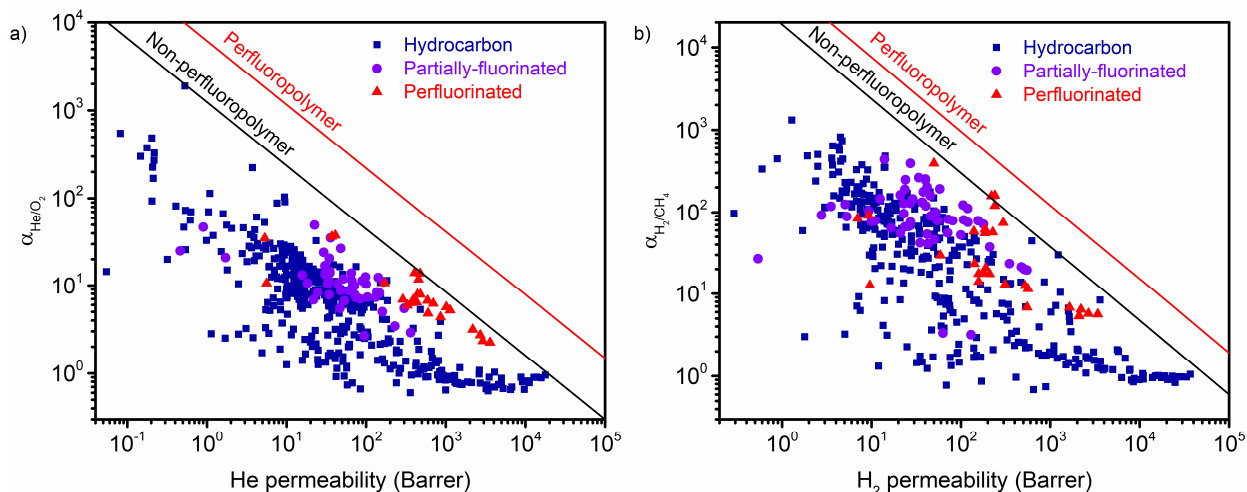


Figure 6: Upper bound plots showing gas pairs where perfluorinated polymers display performance similar to the best non-perfluorinated polymers: a) He/O₂ b) H₂/CH₄

5. Conclusions

The solubility behavior of gases in perfluoropolymers is not considered in the current theoretical framework used to define the Robeson upper bound. This analysis addresses this key limitation by considering distinct theoretical trends in solubility for non-perfluorocarbons and perfluorocarbons. By doing so, new non-perfluoropolymer and perfluoropolymer upper bounds are established and compared to current data. For the five gas pairs examined, it was found that perfluoropolymer data either matched or surpassed the theoretical perfluoropolymer upper bounds established in this work, indicating that the best-performing perfluoropolymers exhibit size-sieving ability equal to or greater than that of the best performing non-perfluoropolymers. Of note, polymers such as Nafion[®] block copolymers, poly(PFMD), poly(PFMMD), and PFMD-PFMMD block copolymers demonstrate the accessible separation performance that can be accessed through improvements in both the diffusivity and solubility terms originally revealed in Freeman's analysis. Additionally, a new trend based on penetrant size and solubility selectivity is presented as a predictive method to estimate non-perfluoropolymer f values, which can then be used to predict both the non-perfluoropolymer and perfluoropolymer upper bound fronts for separations not explicitly considered in this work.

Acknowledgements:

The authors gratefully acknowledge the National Science Foundation Graduate Research Fellowships Program under Grant No. 1122374 for support of A. X. Wu. Additionally, this work was supported through the American Chemical Society Petroleum Research Fund (59256-DNI7).

References:

1. Galizia M, Chi WS, Smith ZP, Merkel TC, Baker RW, Freeman BD. 50th anniversary perspective: polymers and mixed matrix membranes for gas and vapor separation: A review and prospective opportunities. *Macromolecules*. 2017;50(20):7809-7843. doi:10.1021/acs.macromol.7b01718.
2. Sanders DF, Smith ZP, Guo R, Robeson LM, McGrath JE, Paul DR, Freeman BD. Energy-efficient polymeric gas separation membranes for a sustainable future: A review. *Polymer*. 2013;54(18):4729-4761. doi:10.1016/j.polymer.2013.05.075.
3. Sholl DS, Lively RP. Seven chemical separations to change the world. *Nature*. 2016;532(7600):435-437. doi:10.1038/532435a.
4. Baker RW, Low BT. Gas separation membrane materials: A perspective. *Macromolecules*. 2014;47(20):6999-7013. doi:10.1021/ma501488s.
5. Robeson LM. Correlation of separation factor versus permeability for polymeric membranes. *J Mem Sci*. 1991;62(2):165-185. doi:10.1016/0376-7388(91)80060-J.
6. Robeson LM. The upper bound revisited. *J Mem Sci*. 2008;320(1-2):390-400. doi:10.1016/j.memsci.2008.04.030.
7. Freeman BD. Basis of permeability/selectivity tradeoff relations in polymeric gas separation membranes. *Macromolecules*. 1999;32(2):375-380. doi:10.1021/ma9814548.
8. Park HB, Jung CH, Lee YM, Hill AJ, Pas SJ. Polymers with cavities tuned for fast selective transport of small molecules and ions. *Science*. 2007;318(5848):254-258.
9. Ma X, Pinnau I. A novel intrinsically microporous ladder polymer and copolymers derived from 1,1',2,2'-tetrahydroxy-tetraphenylethylene for membrane-based gas separation. *Polym Chem*. 2016;7(6):1244-1248. doi:10.1039/c5py01796c.
10. Carta M, Croad M, Malpass-Evans R, et al. Triptycene induced enhancement of membrane gas selectivity for microporous Tröger's base polymers. *Adv Mater*. 2014;26(21):3526-3531. doi:10.1002/adma.201305783.
11. Bernardo P, Colina CM, Clarizia G, et al. Polymer ultrapermeability from the inefficient packing of 2D chains. *Nat Mater*. 2017;16(9):932-937. doi:10.1038/nmat4939.
12. Yavari M, Fang M, Nguyen H, Merkel TC, Lin H, Okamoto Y. Dioxolane-based perfluoropolymers with superior membrane gas separation properties. *Macromolecules*. 2018;51(7):2489-2497. doi:10.1021/acs.macromol.8b00273.
13. Fang M, He Z, Merkel TC, Okamoto Y. High-performance perfluorodioxolane copolymer membranes for gas separation with tailored selectivity enhancement. *J Mater Chem A*. 2018;6(2):652-658. doi:10.1039/c7ta09047a.

14. Wijmans JG, Baker RW. The solution-diffusion model: a review. *J Mem Sci.* 1995;107(1-2):1-21. doi:10.1016/0376-7388(95)00102-I.
15. Merkel TC. Gas and Vapor Transport Properties of Perfluoropolymers. In: *Materials Science of Membranes for Gas and Vapor Separation.* 2006:251-270.
16. Lanč M, Pilnáček K, Vopička O, et al. Effect of physical aging on the gas transport and sorption in PIM-1 membranes. *Polymer.* 2016. doi:http://dx.doi.org/10.1016/j.polymer.2016.10.040.
17. Tiwari RR, Jin J, Freeman BD, Paul DR. Physical aging, CO₂ sorption and plasticization in thin films of polymer with intrinsic microporosity (PIM-1). *J Mem Sci.* 2017;537(April):362-371. doi:10.1016/j.memsci.2017.04.069.
18. Barrer RM, Rideal EK. Activated diffusion in membranes. *Trans Faraday Soc.* 1939;35:644-656. doi:10.1039/tf9393500644.
19. Cohen MH, Turnbull D. Molecular transport in liquids and glasses. *J Chem Phys.* 1959;31(5):1164-1169. doi:10.1063/1.1730566.
20. Van der Vegt NFA. A molecular dynamics simulation study of solvation thermodynamical quantities of gases in polymeric solvents. *J Mem Sci.* 2002;205(1-2):125-139. doi:10.1016/S0376-7388(02)00071-6.
21. Barrer RM, Skirrow G. Transport and equilibrium phenomena in gas-elastomer systems. I. Kinetic Phenomena. *J Polym Sci.* 1948;3(4):564-575. doi:10.5254/1.3542972.
22. Brandt WW. Model calculation of the temperature dependence of small molecule diffusion in high polymers. *J Phys Chem.* 1959;63(7):1080-1085. doi:10.1021/j150577a012.
23. Robeson LM, Smith ZP, Freeman BD, Paul DR. Contributions of diffusion and solubility selectivity to the upper bound analysis for glassy gas separation membranes. *J Mem Sci.* 2014;453:71-83. doi:10.1016/j.memsci.2013.10.066.
24. Swaidan R, Ghanem B, Pinnau I. Fine-tuned intrinsically ultramicroporous polymers redefine the permeability/selectivity upper bounds of membrane-based air and hydrogen separations. *ACS Macro Lett.* 2015;4(9):947-951. doi:10.1021/acsmacrolett.5b00512.
25. He Y, Benedetti FM, Lin S, et al. Polymers with side chain porosity for ultrapermeable and plasticization resistant materials for gas separations. *Adv Mater.* 2019. doi:10.1002/adma.201807871.
26. Van Amerongen GJ. The permeability of different rubbers to gases and its relation to diffusivity and solubility. *J Appl Phys.* 1946;17(11):972-985. doi:10.1063/1.1707667.
27. Prabhakar RS, Raharjo R, Toy LG, Lin H, Freeman BD. Self-consistent model of concentration and temperature dependence of permeability in rubbery polymers. *Ind Eng Chem Res.* 2005;44(5):1547-1556. doi:10.1021/ie0492909.
28. Krevelen DW van, Nijenhuis K te. *Properties of Polymers.* 4th ed. Amsterdam: Elsevier; 2009. doi:10.1016/B978-0-08-054819-7.00001-7.
29. Smith ZP, Tiwari RR, Dose ME, et al. Influence of diffusivity and sorption on helium and hydrogen separations in hydrocarbon, silicon, and fluorocarbon-based polymers. *Macromolecules.* 2014;47(9):3170-3184. doi:10.1021/ma402521h.
30. Fitch MW, Koros WJ, Nolen RL, Carnes JR. Permeation of several gases through elastomers, with emphasis on the deuterium/hydrogen pair. *J Appl Polym Sci.* 1993;47(6):1033-1046.

- doi:10.1002/app.1993.070470610.
31. Dal-Cin MM, Kumar A, Layton L. Revisiting the experimental and theoretical upper bounds of light pure gas selectivity-permeability for polymeric membranes. *J Mem Sci.* 2008;323(2):299-308. doi:10.1016/j.memsci.2008.06.027.
 32. Robeson LM, Freeman BD, Paul DR, Rowe BW. An empirical correlation of gas permeability and permselectivity in polymers and its theoretical basis. *J Mem Sci.* 2009;341(1-2):178-185. doi:10.1016/j.memsci.2009.06.005.
 33. Breck DW. *Zeolite Molecular Sieves: Structure, Chemistry, and Use.* New York, NY: Wiley; 1974.
 34. Teplyakov V, Meares P. Correlation aspects of the selective gas permeabilities of polymeric materials and membranes. *Gas Sep Purif.* 1990;4(2):66-74. doi:10.1016/0950-4214(90)80030-O.
 35. Reid RC, Prausnitz JM, Sherwood TK. *The Properties of Gases and Liquids.* New York, NY: McGraw Hill Book Co.; 1977.
 36. Bird RB, Stewart WE, Lightfoot EN. *Transport Phenomena.* 2nd ed. New York, NY: John Wiley & Sons Ltd.; 1961.
 37. Shieh JJ, Chung TS. Gas permeability, diffusivity, and solubility of poly(4-vinylpyridine) film. *J Polym Sci Part B Polym Phys.* 1999;37(20):2851-2861. doi:10.1002/(SICI)1099-0488(19991015)37:20<2851::AID-POLB5>3.0.CO;2-U.
 38. Robeson LM, Dose ME, Freeman BD, Paul DR. Analysis of the transport properties of thermally rearranged (TR) polymers and polymers of intrinsic microporosity (PIM) relative to upper bound performance. *J Mem Sci.* 2017;525:18-24. doi:10.1016/j.memsci.2016.11.085.
 39. Matteucci S, Yampolskii Y, Freeman BD, Pinnau I. Transport of Gases and Vapors in Glassy and Rubbery Polymers. In: *Materials Science of Membranes for Gas and Vapor Separation.* 2006:1-47. doi:10.1002/047002903X.ch1.
 40. Mukaddam M, Litwiller E, Pinnau I. Gas sorption, diffusion, and permeation in Nafion. *Macromolecules.* 2016;49(1):280-286. doi:10.1021/acs.macromol.5b02578.
 41. Galizia M, Smith ZP, Sarti GC, Freeman BD, Paul DR. Predictive calculation of hydrogen and helium solubility in glassy and rubbery polymers. *J Mem Sci.* 2015;475:110-121. doi:10.1016/j.memsci.2014.10.009.
 42. Bevington PR, Robinson DK. Data Reduction and Error Analysis for the Physical Sciences, 2nd edn. *Comput Phys.* 1992;7(4):324. doi:10.1063/1.4823194.
 43. Rungta M, Zhang C, Koros WJ. Membrane-based ethylene / ethane separation : The upper bound and beyond. *AIChE Journal.* 2013;59(9):3475-3489. doi:10.1002/aic.
 44. Burns RL, Koros WJ. Defining the challenges for C₃H₆ / C₃H₈ separation using polymeric membranes. *J Mem Sci.* 2003;211(2):299-309.
 45. Baker RW, Lokhandwala KA, He Z, Pinnau I., inventors; Membrane Technology and Research, Inc., assignee. Process, including PSA and membrane separation, for separating hydrogen from hydrocarbons. US Patent 6,183,628. Feb. 6, 2001.
 46. Howard LJ, Howard CR., inventors; Air Products and Chemicals, Inc., assignee. Olefin recovery from olefin-hydrogen mixtures. US Patent 5,634,354. Jun. 3, 1997.

47. Clark Jr. LC, Gollan F. Survival of mammals breathing organic liquids equilibrated with oxygen at atmospheric pressure. *Science*. 1966;152(3730):1755-1756.
48. Merkel TC, Bondar V, Nagai K, Freeman BD, Yampolskii YP. Gas sorption, diffusion, and permeation in poly(2,2-bis(trifluoromethyl)-4,5-difluoro-1,3-dioxole-co-tetrafluoroethylene). *Macromolecules*. 1999;32(25):8427-8440. doi:10.1021/ma990685r.
49. Alentiev AY, Shantarovich VP, Merkel TC, Bondar VI, Freeman BD, Yampolskii YP. Gas and vapor sorption, permeation, and diffusion in glassy amorphous Teflon AF1600. *Macromolecules*. 2002;35(25):9513-9522. doi:10.1021/ma020494f.
50. Scholes CA, Stevens GW, Kentish SE. Membrane gas separation applications in natural gas processing. *Fuel*. 2012;96:15-28. doi:10.1016/j.fuel.2011.12.074.
51. Miyake H, Matsuyama M, Ashida K, Watanabe K. Permeation, diffusion, and solution of hydrogen isotopes, methane, and inert gases in/through tetrafluoroethylene and polyethylene. *J Vac Sci Technol A Vacuum, Surfaces, Film*. 2002;1(3):1447-1451. doi:10.1116/1.572038.
52. Agrinier P, Roizard D, Ruiz-lopez MF, Favre E. Permeation selectivity of gaseous isotopes through dense polymers: Peculiar behavior of the hydrogen isotopes. *J Mem Sci*. 2008;318(1-2):373-378. doi:10.1016/j.memsci.2008.03.011.
53. Leawoods JC, Yablonskiy DA, Gierada DS, Conradi MS, Saam B. Production and MR imaging of the lung. *Concepts Magn Reson*. 2001;13(5):277-293.
54. Sanderson K. Big interest in heavy drugs. *Nature*. 2009;458(7236):269.